Modelling assisted tunneling on the Bloch sphere using the *Quantum Composer*

Jonas Bley¹, Vieri Mattei², Simon Goorney³, Jacob Sherson³, Stefan Heusler ^{4,†}

- ¹Rheinland-Pfälzische Technische Universität Kaiserslautern-Landau
- ²Purdue Department of Physics and Astronomy, West Lafayette, Indiana, US
- ³Department of physics and astronomy, Aarhus University, Denmark
- ⁴Institut für Didaktik der Physik, Westfälische-Wilhems-Universität Münster, Germany
- Correspondence: stefanheusler@uni-muenster.de
- † Current address: Institut für Didaktik der Physik, Wilhelm-Klemm-Str. 10, 48149 Münster, Germany

Received: 25th April 2022 (1st version), 06th December 2022 (2nd version); Accepted: -; Published: -

Abstract: The Bloch-sphere representation is a rather simple geometric model for all possible quantum states of a two-level system. In this article, we propose a simple geometric model for the *time dynamics* of a qubit based on the Bloch-sphere representation. The model can be applied both to time-independent and time-dependent Hamiltonians. As explicit application, we consider time dynamics of a particle in a double-well potential. In particular, we adopt a recent method for off-resonant excitations, the so-called SUPER principle (Swing-UP of the quantum emitter population) in the context of quantum tunneling. We show that the tunneling probability can be enhanced by orders of magnitude when an appropriate oscillation of the potential height is introduced. Driven by a collaborative approach we call *educator-developer dialogue*, an updated version of the software Quantum Composer is presented. Here it is used for educational purposes, to map the two lowest energy states of the 1D-Schrödinger equation to the Bloch sphere representation, leading to a rather clear and intuitive physical picture for the pertinent time dynamics.

Keywords: Multiple representations, Bloch sphere, qubits, tunneling, quantum physics, SUPER principle, Simulation tool

1. Introduction

With the advent of quantum technologies, the importance of two-level systems, also denoted as *qubits*, is increasing not only from a technological, but also from a didactical perspective. In many standard textbooks [1], the topic is adressed in a rather formal manner. Generally speaking, multiple representations are an important tool in science education [2]. This holds true in particular in quantum physics, as the basic concepts are rather abstract and complex. Using the software tool Quantum Composer [3], the mathematical formalism comes to life through interactive graphical visualizations.

In this contribution, as an illustration, we discuss tunneling in a double well as an explict example. In particular, using an update of the Quantum Composer, we apply the so-called Bloch-sphere representation to the double well system.

The Bloch-sphere representation is of particular importance, as it can be applied to all two-level systems, independent of the particular physical interpretation. So far, an explicit geometric model for the time dynamics of qubits on the Bloch sphere has not yet been proposed, presumably due to its triviality: Just choose a rotation axis \vec{n} , which amounts to representing the 2×2 Hamiltonian as $H=\frac{\vartheta}{2}\vec{\sigma}\cdot\vec{n}$. Then, the time dynamics of any initial state $|\psi\rangle=\alpha|0\rangle+\beta|1\rangle$ on the Bloch sphere simply translates to a rotation of this state around the axis \vec{n} on the Bloch sphere. Obviously, there are two eigenstates, namely those

parallel/antiparallel to \vec{n} . This geometric picture is universal in the sense that it is independent of the explicit physical interpretation of the degrees of freedom described by the Hamiltonian.

These multiple representations introduced for Rabi-oscillations can be useful for undergraduate courses on quantum physics. We provide explicit animations and quantum composer files for resonant Rabi-oscillation (Level 1) and off-resonant Rabi-oscillation (Level 2). Next, for graduate level and beyond, we consider a time dependent double-well potential (Level 3).

This paper is organized as follows: In Sect. 2, the Quantum Composer by Quatomic is introduced. In Sect. 3, we review the well-known general theory for Rabi oscillations of two-level systems. In Sect. 4, the tilted double-well potential is introduced as an explicit model system. In Sect. 5 we compare analytic results for the resonant case with numerics from the Quantum Composer (Level 1). In Sect. 6, we do the same for non-resonant Rabi oscillations in the tilted double well (Level 2). In Sect. 7, we introduce the so-called SUPER principle on the Bloch-sphere, which generalizes the simple model for the time dynamics of a qubit to a situation where the rotation axis $\vec{n}(t)$ itself is a certain function of time, allowing for the transition from a given initial state to a given final state with almost 100% probability by adjusting $\vec{n}(t)$ accordingly. In Sect. 8, we apply the SUPER principle, which has been introduced in the context of off-resonant excitations [4], [5] to the situation of quantum tunneling in the tilted double well as model system, which is the main result of the present contribution (Level 3). In Sect. 9, we discuss further extentions and applications of this work, and its possible didactical merits.

2. The Quantum Composer

In this work, we will use the digital tool *Quantum Composer* for numerical simulation of the mechanics of a tilted double well potential. Composer was developed in the group of Prof. Sherson at Aarhus University [6]. Unlike many other fixed-interface applet approaches [7], [8], Composer provides an intuitive and user-friendly re-programmable, node-based graphical interface, as shown in Fig 1. These nodes can be connected to flexibly construct quantum systems which are simulated by the underlying QEngine, a C++ library for the simulation and control of one-dimensional quantum systems [9]. The Quantum Composer can be downloaded for free for most desktop platforms [6]. It is designed for both education (use by teaching staff and students), and for research purposes [10], [11], [12], with a low barrier to entry due to the drag-and-drop nature of the programming.

Due to its hands-on re-programmability, Quantum Composer is uniquely suited to inquiry-based learning (IBL)[13], in which students interact with didactic material through active discovery, questioning, evaluation, and sensemaking. When used for teaching quantum mechanics, IBL has shown potential for improving understanding and reducing overconfidence [14], [15]. Despite this, there are relatively few examples of publicly available resources for inquiry-based quantum mechanics teaching.

There are many simulation and visualization tools [16] already available and they can be invaluable in promoting understanding, interest, and intuition for quantum concepts [17]. However, those which are most widely used for teaching, such as QuVis [7] from and QuILTs [18] offer a fixed set of scenarios covering different phenomena and allow students to vary parameters. While these are effective to enable educators to set up guided and partially inquiry-based teaching situations, they do not allow for truly open and exploratory inquiry, in which the system is entirely set up from scratch by the participants. Thus, such tools may miss out on some of the benefits associated with more open-ended IBL in understanding and promoting scientific thinking [19]. Composer, however, being entirely reprogrammable, allows for teaching material to be developed which can be anywhere on the spectrum of fully guided to completely open-ended and exploratory. An example IBL approach was previously explored using Quantum Composer to devise student exercises based on the Predict, Explore and Revise approach [20].

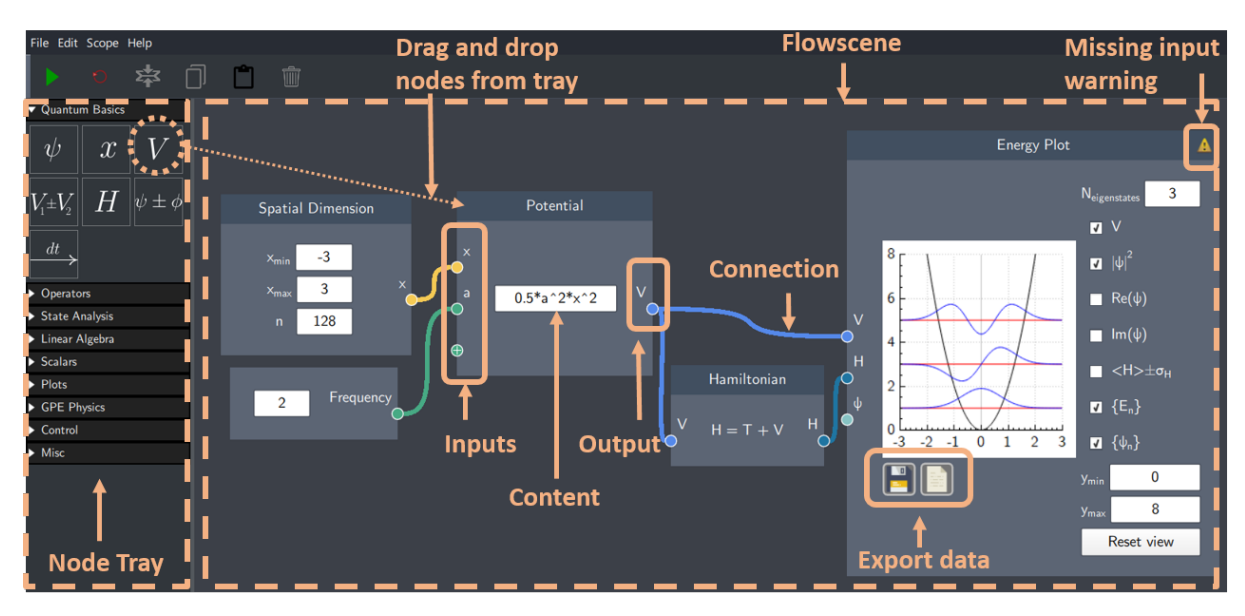


Figure 1. An illustration of the drag-and-drop, node-based, graphical user interface of Quantum Composer.

For researchers, Composer may be useful as a relatively quick and simple means to set up, visualise, and solve analytically intractable quantum systems. The drag-and-drop interface and parameters which can be adjusted on the fly makes it a valuable alternative to more conventional approaches taken by researchers, such as the use of MATLAB or Python code which can be less intuitive to use than the node-based UI of Composer [10], [11]. The tool has previously been used to investigate the dynamics of atoms in atomic lattices [21] and to solve quantum optimal control problems [9], [12].

In the context of this work, however, we wish to highlight another aspect of the Composer re-programmability: the ability of teachers and instructors to seamlessly create custom demonstrators to suit the particular student needs. Here, instructors in advance prepare the relevant .flow files and either use them as lecture demonstrators or distribute them to the students with suitably highlighted experimentation parameters and visualizations preconfigured. In addition, the Composer design team is continually available to support the addition of new interaction and visualisation features. The current work illustrates exactly such interactive collaboration between two instructors (J.B. and S.H.) with the Composer design team resulting in the addition of new features to Composer.

In addition, the Composer design team is continually available to support the addition of new interaction and visualization features. The current work illustrates a form of collaboration between educators (J.B, S.H), and the Composer developers (V.M, S.G, and J.S) which we call *educator-developer dialogue*. In this interactive approach to co-design of educational material, the digital tool is able to act as an instrument to respond to community needs.

There are two possible avenues for this dialogue. The first consists of educators designing material with close input from the developers of the tool. This can be invaluable in identifying and preparing validation criteria, as in reference [3]. The second mechanism, which is demonstrated in this article, is where developers implement new features responding to the needs of the educators, in this case the Bloch-sphere representation. Here we demonstrate the value of Composer by extending the body of existing educational material, using the example of Rabi oscillations in the double well potential. Quantum Composer files are provided for three different levels: Resonant Rabi oscillations (Sect. 5), non-resonant Rabi oscillations (Sect. 6) and Swing Up with the SUPER principle (Sect. 7). The corresponding files can be downloaded from https://physikkommunizieren.de/quantum/tunneling. By combining the

Bloch-sphere representation with the representation of wave functions in the double-well, Composer helps us to develop an intuitive physical picture of the time dynamics in the time-dependent double well using multiple representations. This is the first application of an update of the Quantum Composer incorporating the Bloch-sphere representation, driven by an educator-developer dialogue.

3. A brief review of the general theory of Rabi oscillations

In this section, we briefly review the general theory of Rabi oscillations, which holds for many different applications. One of these applications (the tilted double-well) will be discussed in the following section.

3.1. Time-independent Hamiltonian

Consider a two-level system with states $|L\rangle$ and $|R\rangle$ at energies E_1 , E_2 . Let Δ be the interaction between the two states. This system is described by the following time-independent Hamiltonian

$$H = E_1 |L\rangle\langle L| + E_2 |R\rangle\langle R| + \frac{1}{2}\Delta|L\rangle\langle R| + \frac{1}{2}\Delta|R\rangle\langle L|. \tag{1}$$

Next, we introduce the mean energy $\bar{E} \equiv \frac{1}{2}(E_1 + E_2)$ and the energy splitting $\delta \equiv (E_1 - E_2)$. In matrix notation, the 2 × 2 Hamiltonian can be rewritten as

$$H_{0} = \bar{E} + \frac{1}{2} \begin{bmatrix} \delta & \Delta \\ \Delta & -\delta \end{bmatrix} = \bar{E} + \frac{\sqrt{\delta^{2} + \Delta^{2}}}{2} \begin{bmatrix} \frac{\delta}{\sqrt{\delta^{2} + \Delta^{2}}} & \frac{\Delta}{\sqrt{\delta^{2} + \Delta^{2}}} \\ \frac{\Delta}{\sqrt{\delta^{2} + \Delta^{2}}} & -\frac{\delta}{\sqrt{\delta^{2} + \Delta^{2}}} \end{bmatrix}$$

$$\equiv \bar{E} + \frac{\hbar \omega_{R}}{2} \begin{bmatrix} \cos(2\theta) & \sin(2\theta) \\ \sin(2\theta) & -\cos(2\theta) \end{bmatrix} = \bar{E} + \frac{\hbar \omega_{R}}{2} \vec{\sigma} \cdot \vec{n}.$$
(2)

Here, we introduced the so-called Rabi frequency $\hbar\omega_R = \sqrt{\delta^2 + \Delta^2}$ and the rotation angle θ , which describes the rotation axis of the corresponding time development in the unitary operator

$$U(t) = \exp[-iHt/\hbar] = \exp[-i\bar{E}t/\hbar - i\frac{\omega_R t}{2}\vec{\sigma} \cdot \vec{n}].$$
 (3)

 $\vec{\sigma}$ are the three Pauli-matrices. Indeed, on the Bloch-sphere, this operator generates a rotation of any given initial state around the rotation axis

$$\vec{n} = (\sin(2\theta), 0, \cos(2\theta)) \equiv (\frac{\Delta}{\hbar \omega_R}, 0, \frac{\delta}{\hbar \omega_R}). \tag{4}$$

On the Bloch sphere, the eigenstates point in the $\pm \vec{n}$ directions. In Hilbert space, these eigenstates are given by

$$|+\vec{n}\rangle = \begin{bmatrix} \cos(\theta) \\ \sin(\theta) \end{bmatrix}, \quad |-\vec{n}\rangle = \begin{bmatrix} -\sin(\theta) \\ \cos(\theta) \end{bmatrix}.$$
 (5)

The eigenvalues are given by $E_S = \bar{E} - \frac{1}{2}\omega_R$ and $E_A = \bar{E} + \frac{1}{2}\omega_R$.

In terms of the original basis $|L\rangle$, $|R\rangle$, we find

$$|L\rangle = \cos(\theta)|+\vec{n}\rangle - \sin(\theta)|-\vec{n}\rangle,$$
 (6)

$$|R\rangle = \sin(\theta)|+\vec{n}\rangle + \cos(\theta)|-\vec{n}\rangle.$$
 (7)

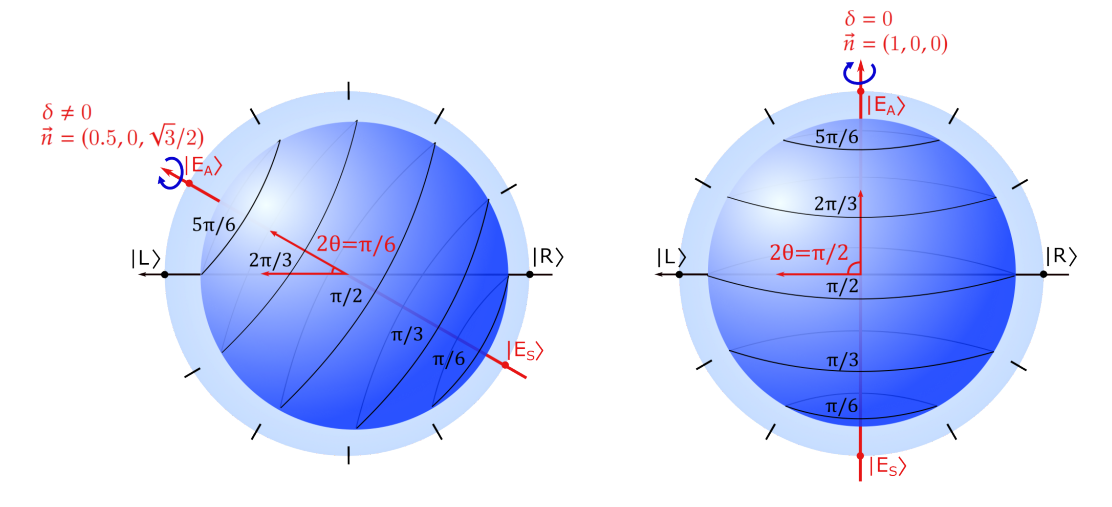


Figure 2. Left: Time development of the state $|L\rangle$ for $2\theta = \pi/6$ (off resonance left), and $2\theta = \pi/2$ (in resonance, right). Only in resonance, the transition probability to state $|R\rangle$ is 100% after a π -flip. The rotation axis \vec{n} , defined by the first two energy-eigenstates of the system E_S and E_A , is shown in red.

For a given initial state $|\psi(0)\rangle$, the fidelity under time development $|\psi(t)\rangle = U(t)|\psi(0)\rangle$ is defined as $F(t) = |\langle \psi(0)|\psi(t)\rangle|^2$. For a general superposition state

$$|\psi_0\rangle = \alpha |+\vec{n}\rangle + \beta |-\vec{n}\rangle \tag{8}$$

with $|\alpha|^2 + |b|^2 = 1$, the time dynamics is given by (up to a global phase)

$$|\psi(t)\rangle = e^{-\frac{i}{2}\omega_R t \vec{\sigma} \cdot \vec{n}} (\alpha | + \vec{n}\rangle + \beta | - \vec{n}\rangle) = e^{+\frac{i}{2}\omega_R t} \alpha | + \vec{n}\rangle + e^{-\frac{i}{2}\omega_R t} \beta | - \vec{n}\rangle$$
(9)

and the fidelity reads

$$F = |\langle \psi(0)|\psi(t)\rangle|^2 = |e^{+i\frac{1}{2}\omega_R t}\alpha^2 + e^{-i\frac{1}{2}\omega_R t}\beta^2|^2 = 1 - 4|\alpha|^2|\beta|^2\sin^2(\frac{\omega_R t}{2}).$$
 (10)

For $|\psi(0)\rangle = |L\rangle$, we obtain

$$F = 1 - \sin^2(\frac{\omega_R t}{2})\sin^2(2\theta). \tag{11}$$

For $2\theta = \pi/2$, the Rabi oscillation is maximal. The fidelity is then given by

$$F = 1 - \sin^2(\frac{\omega_R t}{2}). \tag{12}$$

On the Bloch sphere, there is a simple geometric interpretation for the behaviour of the fidelity. In Fig. 2, we show the rotation axis \vec{n} of the unitary time development, and the orbits of states at angle $\theta = 0$, π

(the eigenstates), and $\theta_k = k\pi/6$, k = 1, ... 5. In analogy to the time dependent system descried in the next section, we call the full Rabi oscillation *resonant* Rabi oscillation, as only for $2\theta = \pi/2$, the transition between the states $|L\rangle$, $|R\rangle$ is certain, as both states are part of the same orbit, leading to (12).

3.2. Time-dependent Hamiltonian: Co-moving frame

The time-independent system described in the previous section is closely related to the corresponding time-dependent Hamiltonian

$$H_1(t) = \begin{bmatrix} E_1 & \frac{1}{2}\Delta e^{i\Omega t} \\ \frac{1}{2}\Delta e^{-i\Omega t} & E_2 \end{bmatrix} = \bar{E} + \frac{1}{2} \begin{bmatrix} \delta & \Delta e^{i\Omega t} \\ \Delta e^{-i\Omega t} & -\delta \end{bmatrix}$$
(13)

with constant Δ . The Schrödinger equation $i\hbar\partial_t\psi=H_1(t)\psi$ can be transformed by the unitary operation $C(t)=\exp\left[-i(\Omega t/2)\sigma_3\right]$ to the co-moving frame $\phi\equiv C(t)\psi$. Note that the rotation axis in this transformation is defined by $|L\rangle,|R\rangle$, not by \vec{n} . Thus, we transform the Schrödinger equation $i\hbar\partial_t\psi=H_1(t)\psi$ to

$$i\hbar\partial_t\phi = (C(t)H_1(t)C^{\dagger}(t) - i\hbar C(t)\partial_t C^{\dagger}(t)))\phi \equiv H_0\phi \tag{14}$$

with

$$H_0 = \bar{E} + \frac{1}{2} \begin{bmatrix} \delta - \hbar\Omega & \Delta \\ \Delta & -\delta + \hbar\Omega \end{bmatrix}. \tag{15}$$

After this transformation, we thus regain the time-independent Hamiltonian H_0 (1) in the co-moving frame with a shift from δ to $\delta - \hbar \Omega$. That is, time dependence $\Delta e^{i\Omega t}$ of the interaction is transformed to a change in the energy shift in the co-moving frame.

While it is interesting to exploit this equivalence further, in particular in the context of off-resonant excitations [4], we will focus on the application of assisted tunneling for the Hamiltonian H_0 (1) in this contribution. in Sect. 8, we will allow for a time dependence in $\Delta(t)$, but we do not consider rapid oscillations of the type $e^{i\Omega t}$.

4. Tunneling in the double well

Quantum tunneling plays a major role in various areas of modern physics. Early applications have been e.g. the calculation of life-times for alpha-decay of nuclei, or for nuclear fusion. In recent time, from a technological perspective, tunneling in solid state physics, and in particular in semiconductor physics and in spintronics [22] are of interest both for the first and in the second quantum revolution. Furthermore, model systems like Bose-Einstein condensates in a double-well potential are part of actual research [23], [24]. In the past decades, periodically driven tunneling systems also have been widely studied [25]. Since tunneling is an important topic in physics since the advent of quantum physics, it is not astonishing that also in physics education, quantum tunneling is part of the standard curriculum not only at university, but also in high school [26]. Thus, it is desirable to explore model systems for quantum tunneling at all levels of education, and also for research. In particular, we want to discuss time-dependent potential wells, which allows for a magnification of the tunneling probability by orders of magnitudes.

Our approach differs from parametric resonance as introduced in [27], as we consider a tilted potential. Thus, we extend the range of applications of tunneling using a coherent excitation scheme using

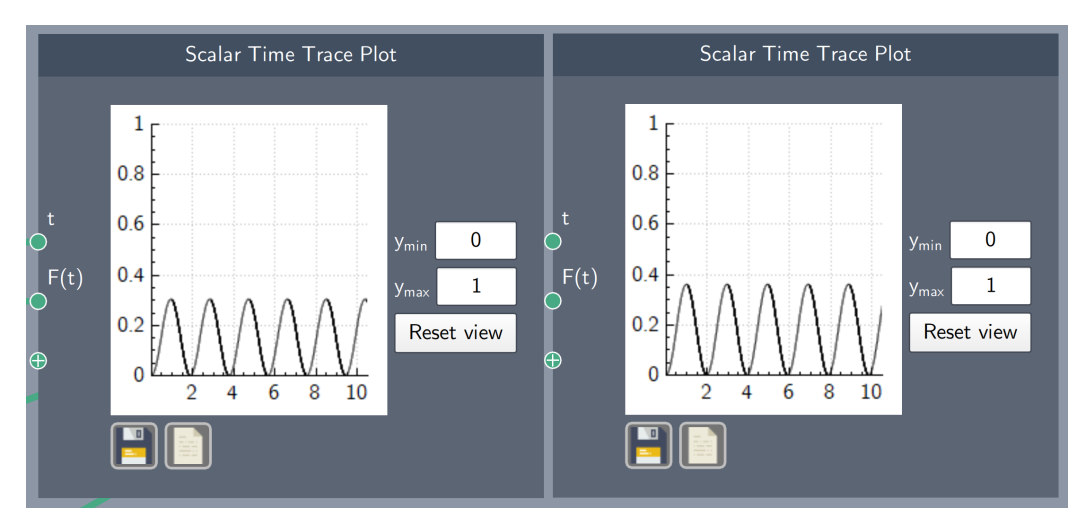


Figure 3. Tunneling probabilities for two different potentials with a=0.7 and $\mu=2.8571$. Left: $\lambda_1=35$, $1-F_1(t)=1-|\langle L_1|\psi_1(t)\rangle|^2$ with $\psi_1(0)=|L_1\rangle=0.9575$ $|E_A\rangle+0.2884i$ $|E_S\rangle$. Right: $\lambda_1=17$,: $1-F_2(t)=1-|\langle L_2|\psi_2(t)\rangle|^2$ with $|L_2\rangle=\psi_1(0)=0.9483$ $|E_A\rangle+0.3172i$ $|E_S\rangle$. These two values of λ will be used to realize assisted tunneling with the SUPER principle which is shown in Sect. 8. The theoretical prediction for the fidelity $1-F(t)=4|\alpha|^2|\beta|^2\sin^2(\omega_Rt/2)$ coincides with the numerical result and cannot be distinguished within the resolution of these plots.

off-resonant pulses - denoted as SUPER principle (Swing-UP of the quantum emitter population) [4]. We translate this idea to the situation of a double well potential and introduce what we call *assisted tunneling*, based on the SUPER principle. In particular, using the Quantum Composer, we show that the tunneling probability can be enhanced by orders of magnitude by introduction of a small oscillation of the potential height, when the oscillation frequency is chosen close to the mean Rabi frequency.

Moreover, from a didacatical point of view, we show that the consequent translation of the tunneling system to the Bloch-sphere representation gives enlightening insights into the physical origin of assisted tunneling.

5. Resonant Rabi oscillations in the double well (Level 1)

As a model for the tunneling system, we consider the double-well potential

$$V(x) = \lambda (x^2 - a^2)^2. {16}$$

First, we want to find a relation between the parameters (δ, Δ) of the general theory of Sect. 3, and the parameters (λ, a) of V(x).

5.1. Analytic results for the transition amplitude Δ for $\mu = 0$

We will calculate $\Delta = \Delta(\lambda, a)$ within this model potential. In the resonance case with $\delta = 0$, we obtain full Rabi oscillation between the symmetric and antisymmetric energy eigenstates $E_S = \bar{E} - \sqrt{\delta^2 + \Delta^2} \to \bar{E} - \Delta$ and $E_A = \bar{E} + \sqrt{\delta^2 + \Delta^2} \to \bar{E} + \Delta$. In this case, the eigenstates are simply given by $|E_S\rangle = 1/\sqrt{2}[|L\rangle + |R\rangle]$ and $|E_A\rangle = 1/\sqrt{2}[|L\rangle - |R\rangle]$, since $\theta = \pi/4$ in (5). In this case, the coupling Δ

can be computed as tunneling amplitude either using WKB or the instanton ansatz. In both approaches, we obtain [28], [29]

$$\frac{1}{2}\Delta(\lambda, a, \mu = 0) = \sqrt{12}\hbar\omega_{H.O.}\sqrt{\frac{S_{\text{inst}}}{2\pi\hbar}}e^{-\frac{S_{\text{inst}}}{\hbar}} = \sqrt{\frac{m^2\omega_{H.O.}^5}{2\pi\lambda}}\exp\left[-\frac{1}{\hbar}(\frac{4}{3}\sqrt{2m\lambda}a^3)\right]. \tag{17}$$

Here, x_{inst} is the so-called instanton solution, a classical path in imaginary time τ connecting the left and the right potential minimum. The instanton action is given by $S[x_{\text{inst}}] = \sqrt{2m} \int \sqrt{V(x)} dx$, leading to

$$S_{\text{inst.}} = \sqrt{2m} \int_{-a}^{+a} \sqrt{\lambda} |x^2 - a^2| dx = \frac{4}{3} \sqrt{2m\lambda} a^3 \equiv \frac{m^2 \omega_{H.O.}^3}{12\lambda}$$
 (18)

with $\omega_{H.O.} = \sqrt{(8a^2\lambda)/m}$. In such a way, we find explicit and analytic expressions for all parameters in the general Hamiltonian (1) in terms of the model potential (16) for the resonance case $\mu = 0$.

6. Non-resonant Rabi oscillations in the tilted double well (Level 2)

Next, we consider the tilted double well, defined by

$$V(x) = \lambda (x^2 - a^2)^2 + \mu x. \tag{19}$$

Let E_1 be the energy of the ground state of the left minimum, and E_2 be the energy of the ground state of the right minimum. Concerning the ground state energies, as (rather bad) approximation, we may compare the potential to the harmonic oscillator. We find in the vicinity of $x \simeq a$ with $y \equiv (x - a)$

$$V(y) \simeq \mu(y+a) + (2a)^2 \lambda y^2 + \dots$$
 (20)

Comparing with the usual energy of the harmonic oscillator, we find $E_1 = \frac{1}{2}\hbar\omega_{H.O.} - \mu a$ and $E_2 = \frac{1}{2}\hbar\omega_{H.O.} + \mu a$ with $\hbar\omega_{H.O.} = \sqrt{(8a^2\lambda/m)}$. Thus, we find in leading order $\delta = (E_1 - E_2) \simeq -2\mu a$. While it is possible to refine the approximations for $E_{1/2}$ using asymptotic series [28], we refrain from doing so here as our main concern is the introduction of assisted tunneling using the Quantum Composer.

We will discuss to what extent we can verify the theory of Rabi oscillations using the Quantum Composer in- and off-resonance. This is the second level of studying Rabi oscillations in the double-well potential with the Quantum Composer. Natural units ($\hbar=1$ and m=1) are used throughout the rest of this paper. Since the eigenvalues for the energy are $E_A=\bar{E}+\frac{1}{2}\sqrt{\Delta^2+\delta^2}$ and $E_S=\bar{E}-\frac{1}{2}\sqrt{\Delta^2+\delta^2}$, we can determine the Rabi frequency $\omega_R=\sqrt{\Delta^2+\delta^2}$ from $E_A-E_S=\omega_R$ and the mean energy by $E_A+E_S=2\bar{E}$. In Fig. 3, we compare the theoretical expression for the fidelity $1-F(t)=4|\alpha|^2|\beta|^2\sin^2(\omega_Rt/2)$ (12) with the results from the quantum composer for two different potentials ($\lambda_1=35,\lambda_2=17$). We find excellent agreement.

In the tilted potential, the instanton calculations that were shown in Sect. 5 for resonant Rabi oscillations are still possible, but much more involved [28]. We will not embark into these troubled waters of theory not to loose track to our main purpose, the introduction of assisted tunneling. However, it would be interesting for future work to link also these analytic results with numerical results obtained with the Quantum Composer. First results and open problems are addressed in the appendix of this work.

To conclude, Rabi oscillations can be studied in an elegant manner with the Quantum Composer for the tilted double well potential and can give valuable insights into some important aspects of the underlying theory.

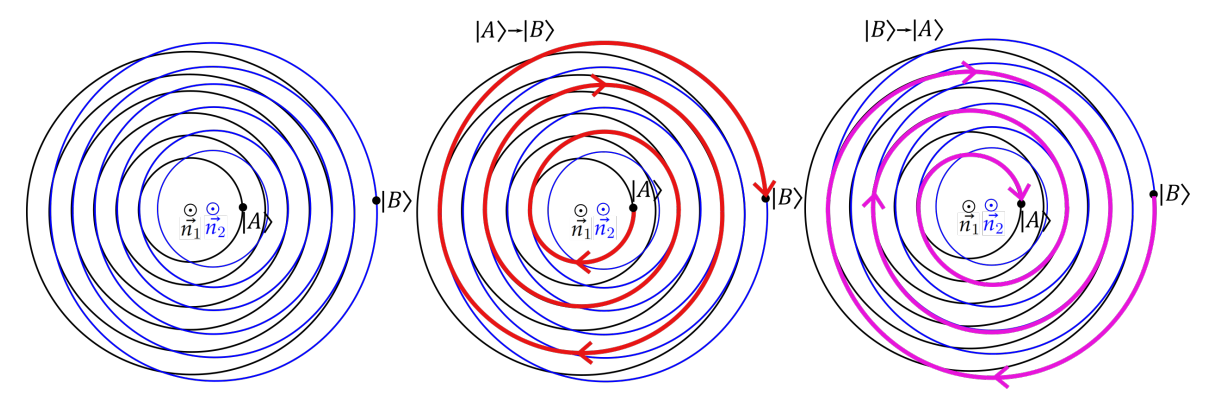


Figure 4. The Swing Up principle illustrated in 2D. Two different potentials V_1 and V_2 have two different rotation axis \vec{n}_1 and \vec{n}_2 pointing towards the reader. By swapping between them, we can go from initial state $|A\rangle$ to state $|B\rangle$ following the red path, or we can go from $|B\rangle$ to $|A\rangle$ following the pink path. When falling out of the swinging rhythm, there is the danger to 'loose track'. Once the state is at $|B\rangle$, if the Swing Up process is not stopped it will follow the pink path and start decaying back to $|A\rangle$. Note that in a full Swing Up, a state viewed in 2D would evolve along the red path and then "back" along the pink path to end in the desired state, orthogonal to the initial state.

7. The SUPER principle on the Bloch sphere (Level 3)

The SUPER principle introduced in [4], [5] is valid in a much broader range of applications than the tunneling system considered in this contribution. For this reason, we start with the rather general 2×2 Hamiltonian

$$H = \bar{E} + \frac{1}{2} \begin{bmatrix} \delta & \Xi(t) \\ \Xi(t) & -\delta \end{bmatrix} = \bar{E} + \frac{\omega_R}{2} \vec{\sigma} \vec{n}(t)$$
 (21)

with $\Xi(t) = \Delta(t)e^{i\Omega t}$, where we encounter two possible time dependencies in $\Xi(t)$. Since the fast oscillation $e^{i\Omega t}$ can be transformed away using the co-moving frame as shown in Sect. 3.2, it is sufficient to consider the time dependence of the amplitude $\Delta(t)$, which translates on the Bloch-sphere to a time dependent rotation axis $\vec{n}(t)$.

The key idea of the SUPER principle is the following: For given rotation axis \vec{n} , the orbit of all initial states under the action of (3) form a "ring system" as shown in Fig. 4. If the rotation axis $\vec{n}(t)$ oscillates between *two different*, but near positions, the time development of an initial state switches between these two "ring systems".

In https://physikkommunizieren.de/quantum/tunneling, we show an animation of the time evolution of the state $|L\rangle$ to the state $|R\rangle$ based on the super principle, applied to the situation shown in Fig. 5. Note that in our specific application, there is no need to perform the transformation to the co-moving frame, as our starting point is the Hamiltonian defined by equation (2).

Indeed, if the oscillation period is chosen nearby the average Rabi frequency of the two different unitary operators (3) with rotation axis \vec{n}_1 and \vec{n}_2 , a "Swing Up" leads to an enhancement of the Rabi amplitude even off-resonance. In a similar manner, also a "Swing Down" can be realized, depending on the initial conditions. This mechanism is valid for any kind of application of Rabi oscillations [4].

8. Assisted tunneling and the SUPER principle

We apply this general SUPER principle to the particular situation of tunneling in a double-well. This is the third, advanced level of studying Rabi oscillations in the double-well potential with the Quantum

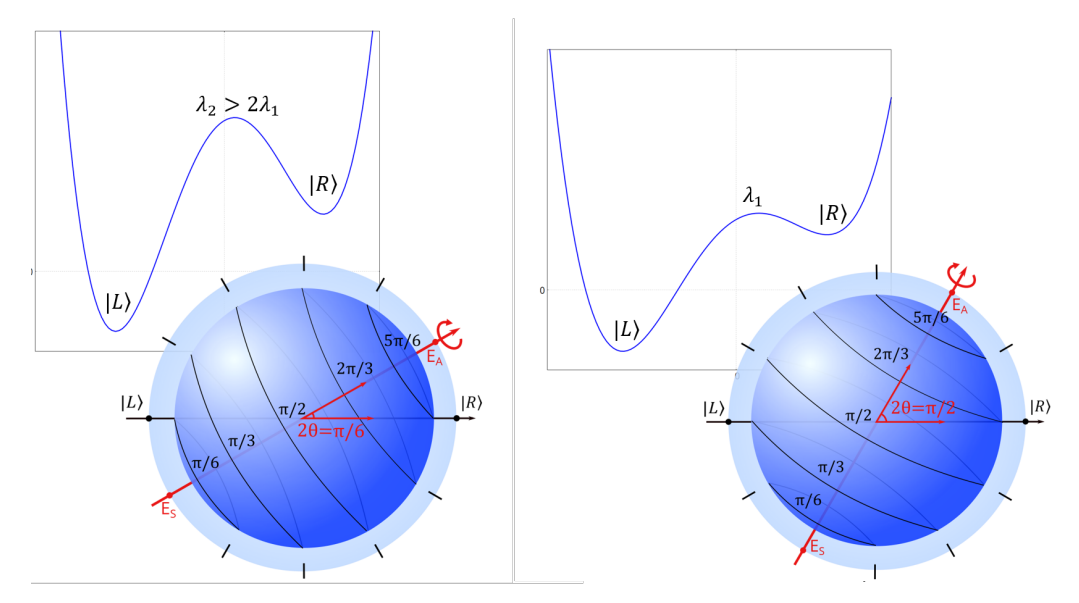


Figure 5. Relation between potential tilt and the corresponding time dynamics on the Bloch sphere. By switching between these two potentials, on the Bloch-sphere, the SWING up mechanism can be realized as shown in Fig. 4

Composer. We consider a situation where the potential height $V(0) = \lambda a^4$ for constant distance a is periodically shifted from a 'high' value to a 'low' value by changing λ . First, we consider the situation where we start in state $|L_1\rangle$ with V_1 or $|L_2\rangle$ with V_2 . For large tilting parameter μ , the tunneling probability to state $|R_1\rangle$ or $|R_2\rangle$ is rather low (Fig. 3). The potentials used, and the initial and desired states are shown in Fig. 6.

Next, we modify the system and allow for an oscillation between V_1 or V_2 , where the potential oscillation frequency is about the mean Rabi frequency. We introduce a smoothstep function to model the transition between the potentials. The result is shown in Fig. 7, confirming the Swing up mechanism, leading to assisted tunneling.

8.1. Practical hints towards realizing assisted tunneling with the Quantum Composer

Assisted tunneling by swapping between two double-well potentials with different barrier heights λ_1 and λ_2 is not an easy task. The parameters have to be chosen carefully to achieve convincing results. We start by choosing two sets of parameters for two different potential functions $V_1(\lambda_1, a, \mu_1) = V_{\text{high}}$ and $V_2(\lambda_2, a, \mu_2) = V_{\text{low}}$, where a is fixed and would typically be given by the physical system, $\lambda_1 \approx 2\lambda_2$ and $\mu_1 = \mu_2$. The closer λ_1 and λ_2 are, the longer the Swing Up will take. This becomes clear when looking at Fig. 4 and is shown in practice by a less steep fidelity graph. Thus, we choose vastly different λ , and $\lambda_1 > \lambda_2$.

The Rabi frequencies $\omega_R^{(1)}$ and $\omega_R^{(2)}$ can be found via $E_A^{(1)} - E_S^{(1)}$ and $E_A^{(2)} - E_S^{(2)}$ respectively. Using (6), we choose as initial state $|L_1\rangle$, given by

$$|L_1\rangle = \sqrt{\frac{\omega_R^{(1)} + 2\mu a}{2\omega_R^{(1)}}} |E_A\rangle + \sqrt{\frac{\omega_R^{(1)} - 2\mu a}{2\omega_R^{(1)}}} |E_S\rangle$$
 (22)

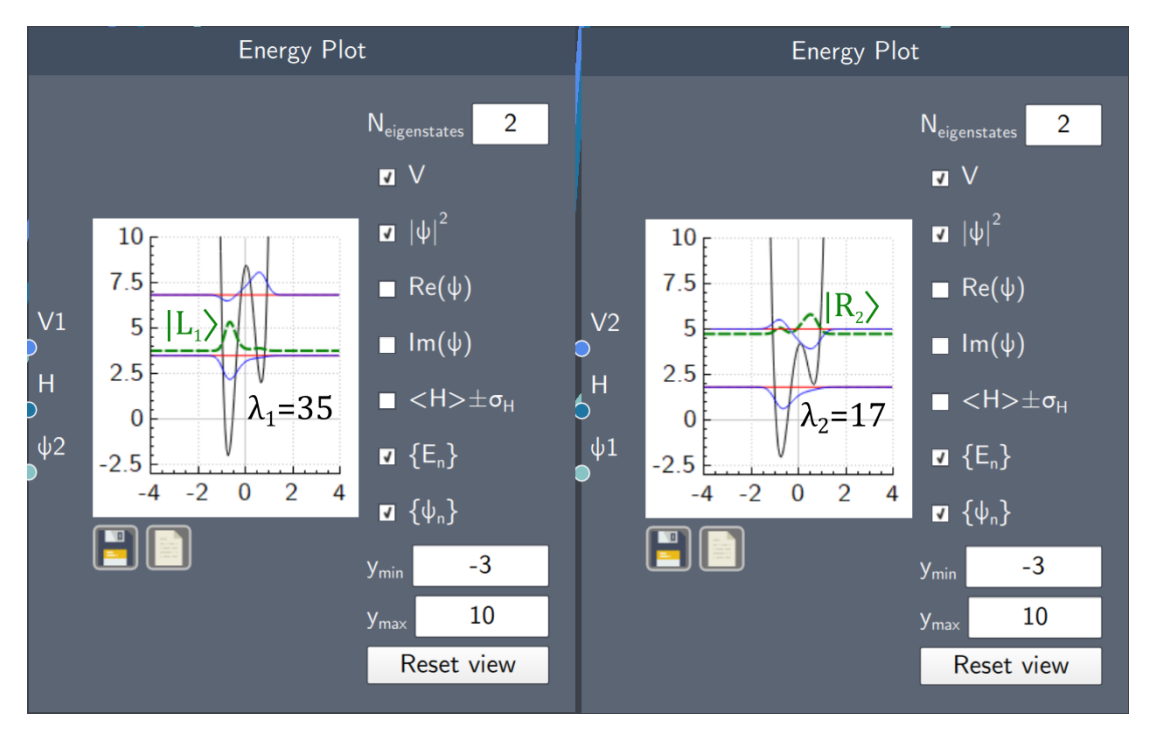


Figure 6. Two potentials ($\lambda_1 = 35$, $a_1 = 0.7$, $\mu_2 = 2.8571$) and ($\lambda_2 = 17$, $a_2 = 0.7$, $\mu_2 = 2.8571$) with the probability density function of the initial state $|L_1\rangle$ and the desired state $|R_2\rangle$. The corresponding Bloch-sphere representation is shown shematically in Fig. 5

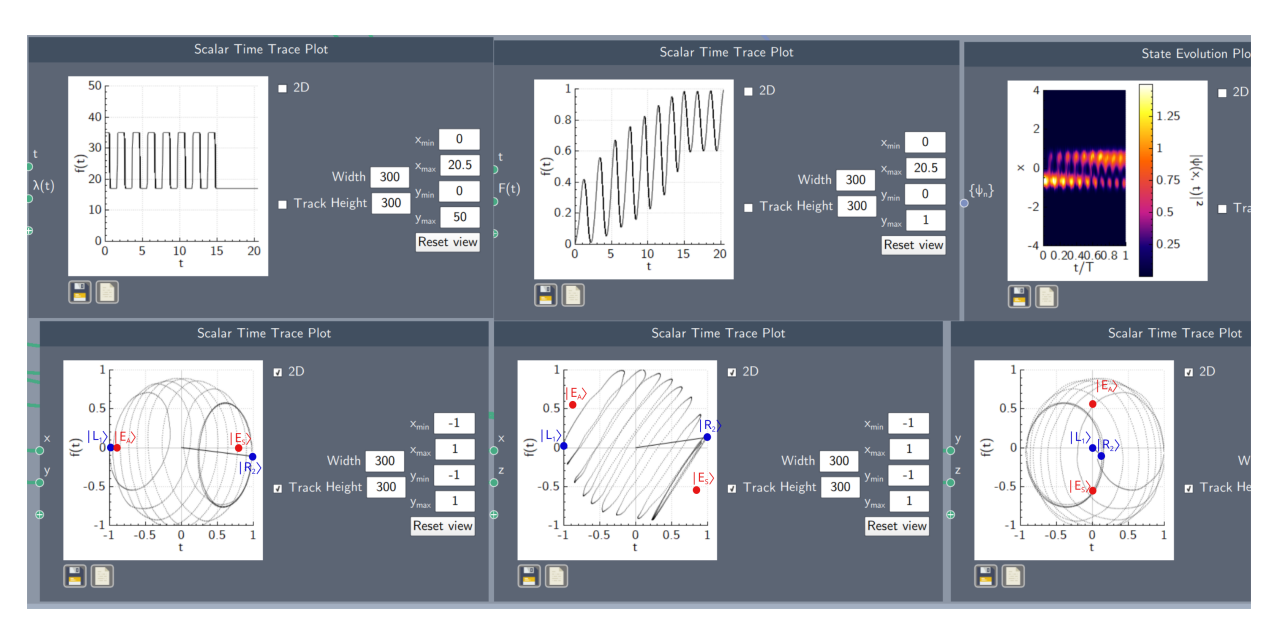


Figure 7. Assisted Tunneling by oscillation between V_1 with $\lambda_1=35$ and V_2 with $\lambda_2=17$ at potential swap time (the time one potential is active before swapping to the next) T/2=1.01. Top Left: Potential barrier height $\lambda(t)$. At 15 time units, the potential was held constant to trap the state at the top. Top Middle: Tunneling probability $F(t)=|\langle \psi(t)|R_2\rangle|^2$ with $\psi(0)=|L_1\rangle$. Top Right: State evolution plot. Bottom: Look at the Bloch Sphere with initial state $|L_1\rangle$, desired state $|R_2\rangle$ and the eigenstates $|E_A\rangle$, $|E_S\rangle$ "from above" (Left), "from the front" (Middle, comparable to Fig. 2) and "from the side" (Right). By periodic oscillation between $\lambda_1=35$ and $\lambda_2=17$, a tunneling probability of over 0.994 was achieved.

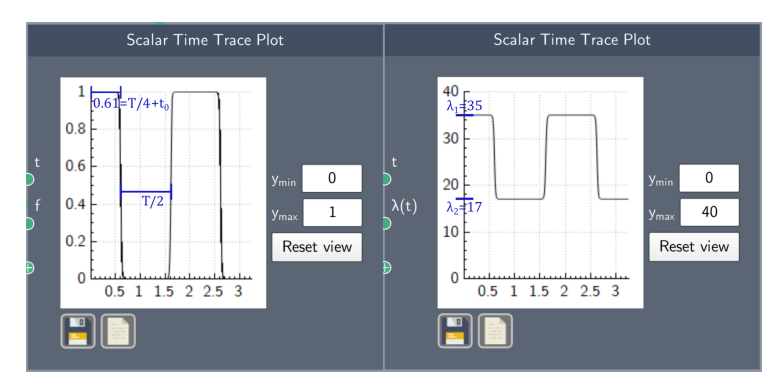


Figure 8. Left: Modulation function $f(t) = \frac{1}{e^{s}g(t)+1}$ where s=20 is the transition slope and $g(t) = -\cos\left(\frac{t-t_0}{T} \cdot \pi\right)$ with potential swap time T/2=1.01 and time offset $t_0=0.1$. Right: Potential barrier height $\lambda(t)=\lambda_1\cdot f(t)+\lambda_2\cdot (1-f(t))$.

while the desired state can be either chosen as

$$|R_1\rangle = -\sqrt{\frac{\omega_R^{(1)} - 2\mu a}{2\omega_R^{(1)}}} |E_A\rangle + \sqrt{\frac{\omega_R^{(1)} + 2\mu a}{2\omega_R^{(1)}}} |E_S\rangle$$
 (23)

or

$$|R_2\rangle = -\sqrt{\frac{\omega_R^{(2)} - 2\mu a}{2\omega_R^{(2)}}} |E_A\rangle + \sqrt{\frac{\omega_R^{(2)} + 2\mu a}{2\omega_R^{(2)}}} |E_S\rangle,$$
 (24)

depending on which of the two potential functions should be final. In our example Swing Up, we chose $|R_2\rangle$.

Next, the potential swap time $T=\frac{2\pi}{\omega}$ (where ω is the potential oscillation frequency) should be chosen. T/2 is the time of one potential being active before swapping to the other. For an optimal fidelity, we observed that T should be about 5% larger than the average Rabi oscillation time T_R of the two potentials, $T_R=4\pi/(\omega_R^{(1)}+\omega_R^{(2)})$. Next, the time offset t_0 at the start of the swing-up can be optimized (see Fig. 8). $T/4+t_0$ is the time of the first swap of the potential.

Using these parameters, we achieve a high fidelity for assisted tunneling in the following manner: First, one should optimize the time offset t_0 for the starting potential swap time T. Next, we optimize T for this offset and repeat. If the resulting fidelity is not satisfying, different values for λ_1 , λ_2 or μ should be chosen. In this manner, a fidelity of over F=0.994 was achieved. The process is challenging in the sense that it is very sensitive to T, t_0 and the potential parameters λ and μ . This could be because the Rabi frequency is not constant during the Swing Up process. Rather, it increases the further $|\psi(t)\rangle$ travels towards $|R\rangle$ as shown in Fig. 9. We have no analytical results that predict this behaviour and can only refer to the numerical results. This can lead to falling out of the swinging rhythm, but can be solved by careful choice of parameters, as shown in this paper.

8.2. Limits of the Bloch-sphere representation for the double-well system

The 2×2 Hamiltonian (21) includes only the two lowest-lying states of an infinite number of eigenstates in the double-well. In this section, we check the validity of the two-level system approximation (22), (23) for the two lowest-lying states localized in the left and the right well, respectively.

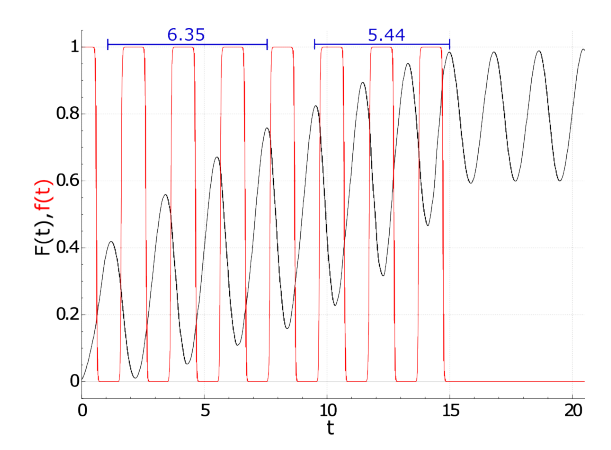


Figure 9. Fidelity F(t) as in Fig. 7, top middle and modulation function f(t) as in Fig. 8 in red. f(t) = 0 corresponds to $\lambda = \lambda_1 = 17$ and f(t) = 1 corresponds to $\lambda = \lambda_2 = 35$. The Rabi frequency increases during the Swing Up process: the first 4 peaks are 6.35 time units apart while the next 4 peaks are only 5.44 time units apart.

In general, these states are a superposition not only of the symmetric and antisymmetric states $|E_A\rangle$, $|E_S\rangle$, but include more states $|\chi\rangle_{R,L}$ with higher energy. Thus, the exact wave functions in position space reads

$$\psi_L^{\text{exact}}(x) = \langle x | L_1 \rangle + \langle x | \chi_L \rangle \equiv \psi_L^{2 \times 2}(x) + \chi_L(x),$$
 (25)

$$\psi_R^{\text{exact}}(x) = \langle x | R_1 \rangle + \langle x | \chi_R \rangle \equiv \psi_R^{2 \times 2}(x) + \chi_R(x).$$
 (26)

These states are fully localized either in the left or the right valley, leading to

$$\int_{-\infty}^{0} |\psi_{L}^{\text{exact}}(x)|^{2} = \int_{-\infty}^{0} |\psi_{L}^{2\times 2}(x)|^{2} + \int_{-\infty}^{0} |\chi_{L}(x)|^{2} = 1, \tag{27}$$

$$\int_0^\infty |\psi_R^{\text{exact}}(x)|^2 = \int_0^\infty |\psi_R^{2\times 2}(x)|^2 + \int_0^\infty |\chi_R(x)|^2 = +1.$$
 (28)

In Fig. 10, we show the expression $1-|\chi_R(x)|^2$ depending on the values for λ , μ . In the region with $\omega_R > 2\mu a$, the deviation from the two-level system is below 5%. Note that for $\omega_R = 2\mu a$, the amplitude for $|E\rangle_S$ in (22) (and $|E\rangle_A$ in (23)) vanishes. After the transition to $\omega_R < 2\mu a$, the amplitude becomes imaginary, and the error increases in an asymmetric manner. While the error stays below 15% for the left valley, it increases to up to 35% in the right valley.

Note that the fidelity F = 0.994 reached by the SUPER-principle for assisted tunneling is much higher. While the visualization of the SUPER principle on the Bloch sphere is rather intuitive and helps understanding the mechanism, the SUPER principle itself is not restricted to the 2×2 level system and indeed includes higher order states during the transition shown in Fig. 7.

8.3. Experimental realisations of the SUPER principle

First experimental realizations of the SUPER principle based on the time-dependent systems of the type (13) have been reported in [5]. In experiment, it is impossible to swap between a "high" value and a "low" value of an electric field with optical laser fields, since modulations at that frequency cannot be

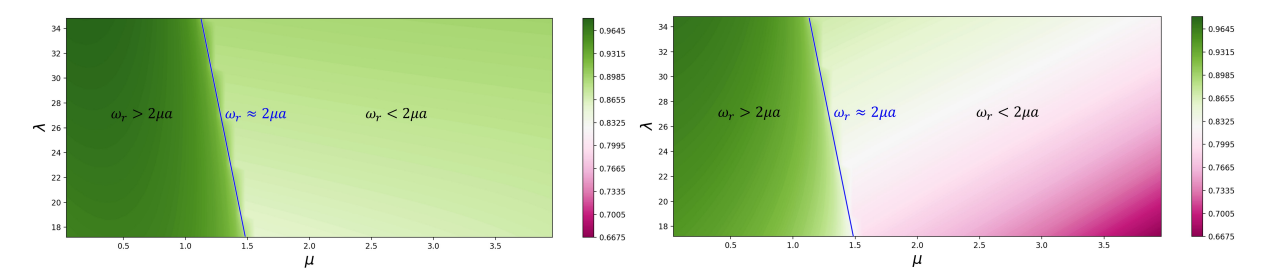


Figure 10. We show deviations of the two-level-system approximation by including contributions of higher order levels as defined by (25), (27). Left: $\int_{-\infty}^{0} \mathrm{d}x |\psi_L^{2\times 2}(x)|^2$ with $|L\rangle$ from eq. (22) for different λ and μ and a=0.7 fixed. Right: $\int_{0}^{\infty} \mathrm{d}x |\psi_R^{2\times 2}(x)|^2$ with $|R\rangle$ from eq. (23). In the region $\omega_R>2\mu a$, the deviation from the two-level system is rather small <10%.

realized. As an alternative, it was shown than to two red-detuned laser pulses which are both off-resonant can lead to the coherent excitation of a quantum dot using the SUPER principle.

In our work, in contrast, we consider the double-well potential as system. In the context of quantum tunneling, it seems possible to find experimental realizations for a "high" value and a "low" value of the potential barrier, as tunneling times can be tuned in orders of magnitude. Explicitly, we may think of a Bose-Einstein condensate trapped in a double-well potential. An experimental realization, where the atoms are magnetically coupled to a single-mode of the microwave field inside a superconducting resonator, has been reported in [30]. By modulating the magnetic field strength, the trap potential could be manipulated to embark for assisted tunneling.

As another model system, we may think of a double-well potential realized for an individual fluxon trapped in a Josephson tunnel junction. Again, parameters of the potential can be manipulated by the strength of a magnetic field [31].

Since the double-well potential is the smallest subpart of the general class of Hubbard-model like system in condensed matter physics, many other appplications of assisted tunneling might be of interest.

9. Outlook and discussion

Our conclusions can be drawn from a didactical perspective, and from the perspective of recent research in applied physics. While periodic oscillations of potentials have already been studied [25], to our knowledge, a systematic enhancement of tunneling using the SUPER-mechanism has not yet been demonstrated. Applications of this mechanism can be of interest in many different areas of physics, as described in Sect. 8.3.

Our main concern however, is physics education: Since the Quantum Composer is available for free, it is possible to discuss Rabi oscillations in an intuitive and direct manner using this powerful modelling tool on almost any computer system. The result of the educator-developer-dialogue is the updated version of the Composer. With this, the explicit visualization of the Bloch sphere dynamics becomes possible. Using the Bloch-sphere representation, the SUPER principle has a simple and general geometric interpretation as shown in Figs. 2, 4 and even a knot theoretic interpretation [32]. Translated back to the double-well, we may apply this mechanism to realize assisted tunneling by introducing an appropriate oscillation of the potential height.

Conceptual clarity and coherence, predictive power and compatibility with existing theories are among the criteria for good scientific models [33]. We believe that our approach fulfils these criteria, and can be considered as a practical and hands-on approach to the important topic of quantum tunneling for science education at all levels of education, and even research.

Explicitly, at high-School, the dependence of the Rabi frequency on the potential parameters (λ, a, μ) can qualitatively be discussed just using the graphical interface provided by the Quantum Composer. On the undergraduate level, the quantitative relations explored in Sect. 4 can be accessed, in particular, the dependence of $S_{\rm inst.} \propto \sqrt{\lambda} a^3$ on the level spacing of the two lowest eigenvalues, $(E_A - E_S) \propto \exp{(-S_{\rm inst.})}$. On the graduate level, assisted tunneling and the SUPER principle can be explored as shown in Sect. 7. Here, analytic results can be used to provide a qualitative understanding of the SUPER-mechanism as shown in Fig. 4. The explicit realization of assisted tunneling can be only realized numerically using the Quantum Composer as described in Sect. 7. All Quantum Composer files we used in our work can be downloaded from the website https://physikkommunizieren.de/quantum/tunneling. Concerning research in physics, still many questions remain open. It would be desirable to understand even better the relation between the numerical results from the Quantum Composer and analytic results, such as 17. Moreover, analytic results for assisted tunneling are not yet available, and it would be desirably to exploit also this approach further analytically in accordance with [34].

On the other hand, for physics education, further empirical studies in relation with learning quantum physics concepts using multiple representations with the Quantum Composer would be desirable.

Even more generally, the simple model for time dynamics of a qubit advocated here in the context of assisted tunneling in fact can be applied in many more situations, since the geometry of the qubit is the same independent of the interpretation of the degrees of freedom considered. Once this general model is established, applications in different areas in physics ranging from solid state physics (e.g. tunneling) to particle physics (e.g. neutrino oscillation) and atomic physics (e.g. absorption/emission) can be understood from this geometric perspective.

10. Appendix: Numerical results for tunneling in the double-well using the Quantum Composer

In this appendix, we check for the validity of the theoretical expression (17) for the transition amplitude. This is the first level of studying Rabi oscillations in the double-well potential with the Quantum Composer. The Quantum Composer uses natural units $\hbar=1$ and m=1 which are used in this section. It follows from (17) that the ratio of the Rabi frequencies coincides with the ratio of the frequencies of the harmonic oscillators,

$$\frac{\Delta_1(S_{\text{inst}} = const, a_1, \lambda_1)}{\Delta_2(S_{\text{inst}} = const, a_2, \lambda_2)} = \frac{\omega_R^{(1)}}{\omega_R^{(2)}} = \frac{\omega_{H.O.}^{(1)}}{\omega_{H.O.}^{(2)}} \simeq \frac{\bar{E}_1}{\bar{E}_2}.$$
 (29)

For example, let $S_{\text{inst}} = \frac{4}{3}\sqrt{2\lambda_1}a_1^3 = 3.7712$ be constant with $\lambda_1 = 45.5625$, $a_1 = 0.6667$. Then, as shown in Tab. 1, we calculate for other pairs of parameters (λ_2, a_2) with identical instanton action S_{inst} the ratios defined in (29). (Explicitly, we work with $\omega_{H.0.}^{(1)} = 2\sqrt{2\lambda_1}a_1 = 12.7286$, $2\overline{E}_1 = E_A^{(1)} + E_S^{(1)} = 11.3446$, $\omega_R^{(1)} = E_A^{(1)} - E_S^{(1)} = 0.5200$). We find excellent agreement, which confirms the functional dependence of $\Delta(a,\lambda)$ as defined in (17), in particular, $S_{\text{inst.}} \propto \sqrt{\lambda}a^3$. Interestingly, even the rather bad approximation $\overline{E} \simeq \omega_{H.O.}/2$ leads to good agreement, as long as the ratio is considered. Using $S_{\text{inst.}} \propto \sqrt{\lambda}a^3$, we may thus explore the effect of the parameters (λ,a) to the energy splitting $E_S - E_A = \Delta(a,\lambda) = \omega_R$ and compare the theory to the numerical results from the Quantum Composer. We may argue that the effect of the distance a in the double-well to the tunneling probability Δ is much larger than the effect of the parameter λ as defined in (16).

On the other hand, we compare the numerical result for the mean energy \bar{E} to the first-order approximation $2\bar{E} \simeq \omega_{H.O.}$ (20). As already discussed, the harmonic oscillator approximation of the potential is rather bad (relative error of about 12%), as shown in Tab 1 when comparing columns 2 and 3.

(λ_2, a_2)	$\omega_{H.O.} = 2\sqrt{2\lambda_2}a_2$	$2\overline{E}_2 = E_A^{(2)} + E_S^{(2)}$	$\omega_R^{(2)} = E_A^{(2)} - E_S^{(2)}$	$\frac{\sqrt{\lambda_1}a_1}{\sqrt{\lambda_2}a_2}$	$\frac{E_A^{(1)} + E_S^{(1)}}{E_A^{(2)} + E_S^{(2)}}$	$\frac{E_A^{(1)} - E_S^{(1)}}{E_A^{(2)} - E_S^{(2)}}$
(4,1)	5.6569	5.04172	0.2312	2.2501	2.2501	2.2491
(0.3512,1.5)	2.5142	2.2409	0.1028	5.0628	5.0625	5.0584
(7,0.9109)	6.8169	6.0752	0.2787	1.8672	1.8674	1.8658
(9,0.8736)	7.4126	6.6067	0.3029	1.7172	1.7171	1.7167
(20,0.7647)	9.6731	8.6209	0.3955	1.3159	1.3159	1.3148

Table 1. First column: Different values of (λ, a) with constant instanton action $S_{\rm inst}$ as defined by (17). Second column: Harmonic oscillator approximation for mean energy (theory), compare (20). Third column: Numerical result for mean energy from quantum composer (with $\hbar=1$). Fourth column: Numerical result for Rabi frequency from quantum composer. Fifth column: Ratio of mean energies with $S_{\rm inst}=const$ from harmonic oscillator approximation (theory). Sixth column: Ratio of mean energies from quantum composer. Seventh column: Ratio of Rabi frequencies from quantum composer. As long as the ratio is considered, we find excellent agreement between theory and numerics, compare also (29), predicting that the ratio of mean energies and Rabi frequencies coincides for $S_{\rm inst}=const$.

While the numerical results for the ratio of two different tunneling amplitudes (17) for constant $S_{\text{inst.}}$ coincides well with the results of the Quantum Composer, we are unable to reproduce the absolute value of (17) including all numerical prefactors using the Quantum Composer. We leave this as an open point for further studies.

11. Acknowledgements

The Aarhus team acknowledged funding from Carlsberg Foundation, Independent Research Fund Denmark (ReGAME) and European Research Council (PQTEI).

The Münster team is grateful to D. Reiter and T. Bracht for valuable discussions.

12. References

- 1. Sakurai, J. Modern quantum mechanics, 2nd edition; Cambridge University Press, 2017.
- 2. Gilbert, J.; Reiner, M.; Nakhleh, M. *Visualization: Theory and Practice in Science Education*; Cambridge University Press, 2008. doi:https://doi.org/10.1007/978-1-4020-5267-5.
- 3. Ahmed, A.; Jensen, J.; Weidner, C.; Sorenson, J.; Mudrich, M.; Sherson, J. Quantum Composer: A programmable quantum visualization and simulation tool for education and research. *American Journal of Physics* **2020**.
- 4. Bracht, T.; Cosacchi, M.; Seidelmann, T.; Cygorek, M.; Vagov, A.; Axt, M.; Heindel, T.; Reiter, D. Swing-Up of Quantum Emitter Population Using Detuned Pulses. *PRX QUANTUM* **2021**, 2. doi:10.1103/PRXQuantum.2.040354.
- 5. Yusuf, K.; Kappe, F.; Remesh, V.; Bracht, T.; Muenzberg, J.; Covre da Silva, S.; Seidelmann, T.; Axt, V.; Rastelli, A.; Reiter, D.; Weihs, G. SUPER Scheme in Action: Experimental Demonstration of Red-detuned Excitation of a Quantum Dot. https://arxiv.org/abs/2203.00712 2022.
- 6. Weidner, C.A.; Ahmed, S.Z.; Jensen, J.H.M.; Sherson, J.F. Publications using Quatomic software. https://www.quatomic.com/composer/. Retrieved 3/25/2021.
- 7. Kohnle, A.; Cassettari, D.; Edwards, T.J.; Ferguson, C.; Gillies, A.D.; Hooley, C.A.; Korolkova, N.; Llama, J.; Sinclair, B.D. A new multimedia resource for teaching quantum mechanics concepts. *American Journal of Physics* **2012**, *80*, 148–153.
- 8. McKagan, S.; Perkins, K.K.; Dubson, M.; Malley, C.; Reid, S.; LeMaster, R.; Wieman, C. Developing and researching PhET simulations for teaching quantum mechanics. *American Journal of Physics* **2008**, *76*, 406–417.

- 9. Sørensen, J.J.; Jensen, J.; Heinzel, T.; Sherson, J.F. QEngine: A C++ library for quantum optimal control of ultracold atoms. *Computer Physics Communications* **2019**, 243, 135–150.
- 10. Weidner, C.A.; Ahmed, S.Z.; Jensen, J.H.M.; Sherson, J.F. Research using Quatomic software. https://www.quatomic.com/composer/research. Retrieved 27/11/2021.
- 11. Ahmed, A.; Jensen, J.J.; Weidner, C.A.; Sørensen, J.J.; Mudrich, M.; Sherson, J.F. Quantum Composer: A programmable quantum visualization and simulation tool for education and research. *Arxiv*, *physics.ed-ph* **2020**.
- 12. Jensen, J.; Sørensen, J.J.; Mølmer, K.; Sherson, J.F. Time-optimal control of collisional $\sqrt{\text{SWAP}}$ gates in ultracold atomic systems. *Phys. Rev. A* **2019**, *100*, 052314.
- 13. Bell, R.; Bianchi, H. The Many Levels of Inquiry. Science & Children 2008, 46(2).
- 14. Rodriguez, L.V.; van der Veen, J.T.; Anjewierden, A.; van den Berg, E.; de Jong, T. Designing inquiry-based learning environments for quantum physics education in secondary schools. *Phys. Educ.* **2020**, *55*.
- 15. Testa, I.; Colantonio, A.; Galano, S.; Marzoli, I.; Trani, F.; Scotti di Uccio, U. Effects of instruction on students' overconfidence in introductory quantum mechanics. *Phys. Rev. Phys. Educ. Res.*, **2020**, *16*, 010143.
- 16. Seskir, Z.C.e.a. Quantum games and interactive tools for quantum technologies outreach and education. *Opt. Eng.* **2022**, *61*(*8*), 081809.
- 17. Goorney, S.; Foti, C.and Santi, L.; Sherson, J.; Yago Malo, J.; Chiofalo, M. Culturo-scientific storytelling. *Education Sciences* **2022**, *12*(7), 474.
- 18. Singh, C. Interactive learning tutorials on quantum mechanics. *American Journal of Physics* **2008**, 76(4), 400–405.
- 19. Kuhn, D. What is Scientific Thinking and How Does it Develop?, in The Wiley-Blackwell Handbook of Childhood Cognitive Development; Blackwell Publishing Ltd, 2008. doi:https://doi.org/10.1002/9781444325485.ch19.
- 20. Ahmed, A.; Weidner, C.A.; Jensen, J.J.; Sherson, J.F.; Lewandowski, H.J. Student use of a quantum simulation and visualization tool. *Eur. J. Phys.* **2022**, 43.
- 21. Elíasson, O.; Laustsen, J.S.; Heck, R.; Müller, R.; Arlt, J.J.; Weidner, C.A.; Sherson, J.F. Spatial tomography of individual atoms in a quantum gas microscope. *Phys. Rev. A* **2020**, *102*, 053311. doi:10.1103/PhysRevA.102.053311.
- 22. Miao, G. Reports on Progress in Physics Tunneling path toward spintronics. Rep. Prog. Phys. 2011, 74.
- 23. Ananikian, D.; Bergeman, T. Gross-Pitaevskii equation for Bose particles in a double-well potential: Two-mode models and beyond. *Physical Review A* **2006**, *7*3.
- 24. Devoret, M.H.; Wallraff, A.; Martinis, J.M. Superconducting Qubits: A Short Review. *arXiv: Mesoscale and Nanoscale Physics* **2004**.
- 25. Grifoni, M.; Hänggi, P. Driven quantum tunneling. *Phys. Rep.* **1998**, 304.
- 26. Stademann, K. Analysis of secondary school quantum physics curricula of 15 different countries: Different perspectives on a challenging topic. *PHYSICAL REVIEW PHYSICS EDUCATION RESEARCH* **2019**, *15*. doi:10.1103/PhysRevPhysEducRes.15.010130.
- 27. Peano, V.; Marthaler, M.; Dykman, M.I. Sharp Tunneling Peaks in a Parametric Oscillator: Quantum Resonances Missing in the Rotating Wave Approximation. *Phys. Rev. Lett.* **2012**, *109*, 090401. doi:10.1103/PhysRevLett.109.090401.
- 28. Rastelli, G. Semi-classical formula for quantum tunneling in asymmetric double-well potentials. *Phys RevA*. **2012**, *86*. doi:10.1103/PhysRevA.86.012106.
- 29. Coleman, S. *Aspects of Symmetry: Selected Erice Lectures*; Cambridge Univ. Press, 1985. doi:10.1017/CBO9780511565045.
- 30. Ng, H.; Chu, S. Steady-state entanglement in a double-well Bose-Einstein condensate through coupling to a superconducting resonator. *Phys. Rev. A* **2011**, *84*. doi:10.1103/PRXQuantum.2.040354.
- 31. Monaco, R. Engineering Double-Well Potentials with Variable-Width Annular Josephson Tunnel Junctions. *Journal of Physics: Condensed Matter* **2016**, *28*.
- 32. Heusler, S.; Ubben, M. A Haptic Model of Entanglement, Gauge Symmetries and Minimal Interaction Based on Knot Theory. *Symmetry* **2019**, *11*, 1399. doi:10.3390/sym11111399.
- 33. Pluta, W.; Chinn, C.; Duncan, R. Learners' epistemic criteria for good scientific models. *J. Res. Sci. Teach.* **2011**, 48.

34. Shi, Z.; Chen, Y.; Qin, W.; Xia, Y.; Yi, X.; Zheng, S.; Nori, F. Two-level systems with periodic N-step driving fields: Exact dynamics and quantum state manipulations. *PHYSICAL REVIEW A* **2021**, *104*. doi:10.1103/PhysRevA.104.053101.